This is an open access article published under an ACS AuthorChoice License, which permits copying and redistribution of the article or any adaptations for non-commercial purposes.

ACS OMEGA

Article

Cite This: ACS Omega 2018, 3, 8992−9002

http://pubs.acs.org/journal/acsodf

Nonconjugated Fluorescent Molecular Cages of Trinuclear Fluoroborate Complexes with Salicylaldehyde-Based Schiff Base Ligands

Xiaohong Zhang,[†,§] Jun Shi,[‡,§] Jintong Song,[†] Man Wang,[†] Xuemei Xu,[†] Lang Qu,[†] Xiangge Zhou,[†] and Haifeng Xiang*[,†]

[†]College of Chemistry, Sichuan University, Chengdu 610041, China

[‡]Department of Cardiovascular Surgery, West China Hospital, Sichuan University, 37 Guoxue Xiang Street, Chengdu 610041, Sichuan, China

Supporting Information

ABSTRACT: Fluorescent organic materials are commonly π-conjugated planar molecules. In the present work, however, we report a novel class of nonconjugated fluorescent molecular cages of trinuclear fluoroborate complexes (nine samples) with salicylaldehyde-based Schiff base ligands. Owing to the stress from lone pair electrons of N atom in the triethylamine bridge, these B(III) complexes exhibit unusual enantiomers with a tripodlike side-single-opening structure. They emit blue, green, and red emission with large Stokes shifts (up to 159 nm) and high fluorescence quantum yields in both solution (up to 0.24) and solid state (up to 0.25), which might contribute to their strong intramolecular hydrogen bonds and weak intermolecular and intramolecular π−π interactions. Combining their advantages of nonconjugation and biocompatibility, these flexible complexes have potential applications in living cell imaging and anion hosts. We have examined the inherent relationships between their chemical structures and emission properties and afforded a new stage for the design of nonconjugated fluorescent fluoroborate complexes.

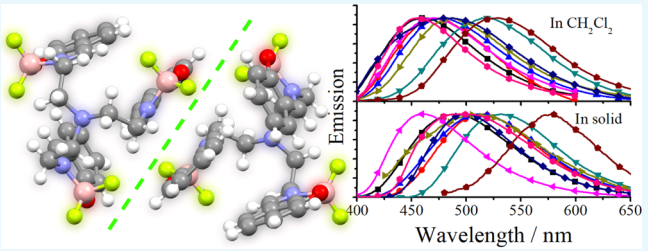

INTRODUCTION

The development of innovative organic luminescent materials[1] recently has attracted intense interest due to their wide range of applications in optical probes,[2−8] organic light-emitting diodes,[9−13] light-emitting electrochemical cells,[14,15] and cell imaging.[16−19] In general, organic luminescent materials with π-conjugated planar and rigid structures are extremely susceptible to the problems of emission "aggregation-caused quenching" (ACQ)[20,21] and synthesis difficulty and solubility. On the other hand, nonconjugated materials with better solubility, higher flexibility, lower cost, lower cytotoxicity, better biocompatibility, and naturally occurring[22] are usually known as nonemissive materials. Until recently, there are only a limited number of fluorescent pure organic nonconjugated materials[23−26] that emit ultraviolet (UV) and blue aggregation-induced emission (AIE).[23,27,28] Our research group also just reported that some free ligands of nonconjugated bi- and trisalicylaldehyde-based Schiff bases (SSBs) show fine-tuned red−green−blue (RGB) AIE properties.[29−31]

Among the numerous classes of fluorescent materials, boron(III) complexes have perhaps the highest potential and have spectacularly risen in popularity because of their very promising advantages of relatively high molar absorption coefficients (ε), fine-tuned emission bands (λ_{em}) with high fluorescence quantum yields (Φ), and photostability. This family of dyes includes not only well-known boron dipyrromethene[32−35] but also its derivatives based on N^O,[36−39] N^C,[40,41] and O^O[42−44] chelates. Two major drawbacks of these B(III) complexes are their problems of ACQ and self-absorption. The ACQ problem of B(III) complexes is mostly caused by intermolecular π−π stacking interactions between π-conjugated planar molecules, and the self-absorption problem results from very narrow Stokes shifts between absorption and emission spectra. Our research works continually focus on the synthesis, optical properties, and sensing applications of SSBs[29−31,45−47] and their Zn(II), Cu(II), Al(III), and Pt(II) complexes.[48−51] In the literature, there are many examples of fluorescent B(III) complexes with N^O-bidentate SSB ligands (Figure 1a,b).[52−61] However, most of them are mononuclear or binuclear B(III) complexes (Φ up to 0.90 in solution)[58] with π-conjugated planar molecular structures and often suffer the ACQ problem. Reported π-conjugated fluorescent trinuclear B(III) complexes[52,58] and nonconjugated fluorescent binuclear B(III) complexes[60,61] are still rare. It is interesting that free ligands of π-conjugated bi-/tri-SSBs[58] and nonconjugated bi-SSBs[29] are usually AIE-active

Received: July 1, 2018
Accepted: July 31, 2018
Published: August 13, 2018

 © 2018 American Chemical Society

DOI: 10.1021/acsomega.8b01504
ACS Omega 2018, 3, 8992−9002

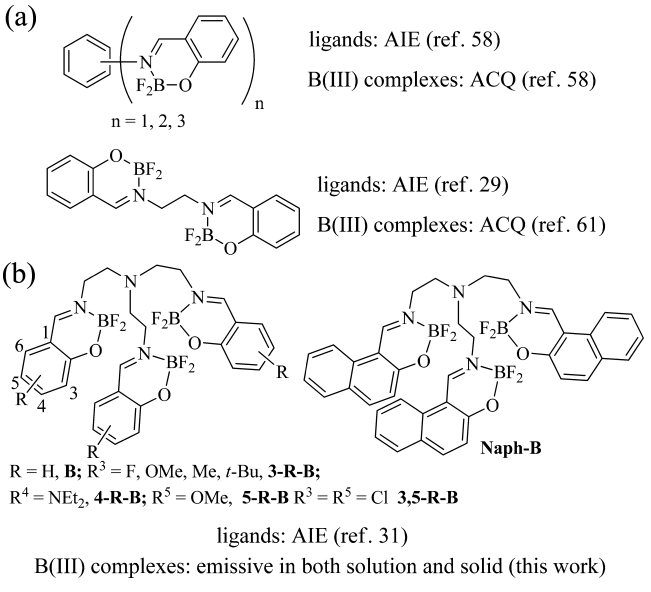

Figure 1. Reported fluorescent B(III) complexes (a) with π-conjugated and nonconjugated N^O-bidentate SSB ligands. Trinuclear fluoroborate complexes (b) in this work.

materials, but their B(III) complexes are ACQ-active materials (Figure 1a).[58,61] The free ligands of nonconjugated trimethylamine-linking tri-SSBs are AIE-active materials as well (Figure 1b),[31] and we wonder if their trinuclear B(III) complexes are AIE- or ACQ-active materials. Herein, we demonstrate a novel class of trinuclear fluoroborate complexes with nonconjugated trimethylamine-linking tri-SSB ligands (nine samples, Figure 1b) that exhibit unusual enantiomers with a tripodlike side-single-opening structure and emit strong RGB fluorescence in both solution and solid state with large Stokes shifts.

RESULTS AND DISCUSSION

Synthesis and Characterization. The free tri-SSB ligands were reasonably easy to be synthesized by the condensation of primary triethylamine with 3 equiv of salicylaldehyde precursor in ethanol under refluxing condition.[31] The B(III) complexes were prepared by using $BF_3{-}OEt_2$ and tri-SSB ligands in toluene at 60 °C with excellent yields (70−88%).[61] Most of the B(III) complexes have a bad solubility in petroleum ether, hexane, and water but a good solubility in CH_3CN, CH_2Cl_2, dimethylformamide, and dimethyl sulfoxide (DMSO). All of the complexes are stable under air. For most of the complexes, good-quality single crystals could be obtained by the method of slow solvent diffusion/evaporation (CH_2Cl_2/hexane). The B(III) complexes are not new,[62] but we report our systematic studies of the inherent relationships between their chemical structures and fluorescent properties and the potential application in ion sensing.

Photophysical Properties. Table 1 lists the UV−visible absorption and fluorescence data of all synthesized B(III) complexes at room temperature. To gain insight into the nature of the excited states and transitions, density functional theory (DFT) and time-dependent-DFT (TD-DFT) calculations were also carried out for **B** with the Gaussian 09 program package (B3LYP 6-31G(d,p)). The computational absorption spectrum is virtually identical to the experimental absorption spectrum (Figure 2). The lower energy absorption band of **B** (λ_{abs} = 347 nm in CH_2Cl_2) is reproduced well by the computation, which predicts one absorption peak at 336 nm. The lower energy absorption is contributed by $S_0 \rightarrow S_1$ (353 nm, oscillator strength f_{OSC} = 0.0386, the highest occupied molecular orbital (HOMO) → lowest unoccupied molecular orbital (LUMO), 74%; HOMO − 1 → LUMO, 18%; HOMO → LUMO + 1, 6%) and $S_0 \rightarrow S_2$ (347 nm, f_{OSC} = 0.0350, HOMO − 1 → LUMO, 50%; HOMO → LUMO + 1, 27%; HOMO − 1 → LUMO + 1, 11%; HOMO → LUMO, 5%). The energy-level and orbital isosurface diagrams of **B** (Figure 2) reveal that the HOMO and HOMO − 1 of **B** are composed primarily of not only two π-conjugated units of iminomethylphenol but also the nonconjugated triethylamine bridge, which might contribute to the electron-donating nature of triethylamine. On the contrary, its LUMO and LUMO + 1 are mainly made up of the π-functions of iminomethylphenol units rather than the triethylamine bridge. Therefore, the lower energy absorption can mainly be assigned to the intraligand $\pi \rightarrow \pi^*$ transition involving molecular orbitals essentially localized on the iminomethylphenol units and intramolecular charge transfer (ICT, $n \rightarrow \pi^*$) transition from electron-donating trimethylamine (lone pair electrons of N atom) to the π-conjugated iminomethylphenol units. The difluoroborate units have little contribution to the lower energy absorption. For free ligand of tri-SSB,[31] however, the lower energy absorption was mostly contributed by $n \rightarrow \pi^*$ transition from electron-donating trimethylamine to the π-conjugated iminomethylphenol units. These computational data are consistent with the fact that **B** (λ_{abs} = 346 nm in MeCN) has a red-shifted absorption spectrum compared with the tri-SSB ligand (λ_{abs} = 314 nm in MeCN).

The absorption spectra of all of the B(III) complexes in pure organic solvent of CH_2Cl_2 (2.0×10^{-5} mol dm^{-3}) are given in Figure 3. The introduction of steric hindrance −Me (**3-Me**, λ_{abs} = 355 nm in MeCN) or −*t*-butyl (**3-*t*-Bu**, λ_{abs} = 353 nm) (Figure 3 and Table 1) substituents to the simplest **B** (λ_{abs} = 347 nm) has little effect on absorption spectra. However, except the presence of electron-accepting −F (**3-F-B**, λ_{abs} = 353 nm), the presence of electron-accepting −Cl (**3,5-Cl-B**, λ_{abs} = 369 nm), electron-donating −OMe (**3-OMe-B**, λ_{abs} = 374 nm; **5-OMe-B**, λ_{abs} = 388 nm), $-NEt_2$ (**4-NEt_2-B**, λ_{abs} = 375 and 347 nm), or π-extended system (**Naph-B**, λ_{abs} = 370 and 332 nm) induces obvious red shifts in absorption spectra. It is obvious that the UV absorption behavior of **4-NEt_2-B** solution is unique, which might be contributed by the strong electron-donating property of NEt_2 groups.

As our previous report,[31] free ligands of tri-SSBs showed very weak blue fluorescence in the dilute organic solvents because their intramolecular rotations (IRs) of C−N and C−C single bonds in the central triethylamine bridge provide a possible way to nonradiatively annihilate their excited states and result in the absence of fluorescence consequently. However, it is unexpected that most of the B(III) complexes exhibit strong fluorescence in both solid and pure organic solvent of toluene, CH_2Cl_2, or acetone (Table 1 and Figures 4 and 5). As an example, **B** emits strong blue fluorescence (λ_{em} = 455−461 nm, Φ = 0.061−0.083) with large Stokes shifts (up to 110 nm) in low polar solvent of toluene, CH_2Cl_2, or acetone. The absence of fluorescence in the solution of free tri-SSB ligand contributed to the nature of $n \rightarrow \pi^*$ transition and IRs;[31] on the other hand, the transition of **B** originate from not only $n \rightarrow \pi^*$ but also $\pi \rightarrow \pi^*$ transition (Figure 2), which would help achieve strong fluorescence in both solution and solid state (see the later discussion). In addition, the B(III)

DOI: 10.1021/acsomega.8b01504
ACS Omega 2018, 3, 8992−9002

Table 1. Photophysical Data of the B(III) Complexes at Room Temperature

	medium	λ_{abs}/nm (ε/dm^3 mol^{-1}cm^{-1})	λ_{em}/nm	Stokes shift/nm	Φ
B	toluene	280(1.78 × 10^4); 346(1.28 × 10^4)	455	109	0.061
	CH_2Cl_2	266(4.98 × 10^4); 347(1.61 × 10^4)	459	112	0.064
	ethanol	263(3.75 × 10^4); 347(1.23 × 10^4)	461	114	0.032
	acetone	343(1.25 × 10^4)	461	118	0.083
	MeCN	262(4.89 × 10^4); 346(1.37 × 10^4)	457	111	0.012
	DMSO	270(4.26 × 10^4); 345(1.72 × 10^4)	458	113	0.001
	solid		489		0.071
3-F-B	toluene	283(2.15 × 10^4); 353(9.85 × 10^3)	476	123	0.037
	CH_2Cl_2	265(4.74 × 10^4); 353(1.08 × 10^4)	470	117	0.034
	ethanol	269(5.08 × 10^4); 349(1.14 × 10^4)	475	126	0.014
	acetone	355(1.05 × 10^4)	475	120	0.035
	MeCN	265(5.22 × 10^4); 344(1.34 × 10^4)	467	123	0.003
	DMSO	275(5.36 × 10^4); 345(1.59 × 10^4)	479	134	0.002
	solid		518		0.053
3-Me-B	toluene	283(3.11 × 10^4); 358(1.33 × 10^4)	475	117	0.10
	CH_2Cl_2	266(6.38 × 10^4); 355(1.46 × 10^4)	477	122	0.074
	ethanol	271(4.87 × 10^4); 355(1.25 × 10^4)	479	124	0.058
	acetone	358(1.26 × 10^4)	474	116	0.077
	MeCN	274(4.69 × 10^4); 353(1.32 × 10^4)	479	126	0.033
	DMSO	277(6.02 × 10^4); 353(1.76 × 10^4)	476	123	0.006
	solid		513		0.064
3-OMe-B	toluene	291(1.25 × 10^4); 379(6.00 × 10^3)	512	133	0.015
	CH_2Cl_2	277(5.34 × 10^4); 374(1.74 × 10^4)	517	143	0.013
	ethanol	277(7.70 × 10^4); 368(1.45 × 10^4)	519	151	0.015
	acetone	358(2.35 × 10^4)	519	161	0.014
	MeCN	278(7.66 × 10^4); 366(1.58 × 10^4)	525	159	0.008
	DMSO	287(7.43 × 10^4); 366(2.26 × 10^4)	521	155	0.007
	solid		532		0.030
3-*t*-Bu-B	toluene	279(5.73 × 10^4); 353(1.29 × 10^4)	464	111	0.15
	CH_2Cl_2	270(4.86 × 10^4); 353(1.43 × 10^4)	470	117	0.13
	ethanol	269(3.35 × 10^4); 356(1.05 × 10^4)	469	113	0.099
	acetone	353(1.26 × 10^4)	464	111	0.14
	MeCN	270(3.93 × 10^4); 352(1.28 × 10^4)	477	125	0.052
	DMSO	279(4.75 × 10^4); 352(1.96 × 10^4)	472	120	0.008
	solid		461		0.16
3,5-Cl-B	toluene	289(1.25 × 10^4); 373(1.11 × 10^4)	492	119	0.033
	CH_2Cl_2	270(3.15 × 10^4); 369(1.05 × 10^4)	488	119	0.03
	ethanol	270(3.66 × 10^4); 365(1.26 × 10^4)	489	124	0.005
	acetone	373(1.10 × 10^4)	490	117	0.031
	MeCN	270(3.62 × 10^4); 363(1.40 × 10^4)	490	127	0.001
	DMSO	275(3.46 × 10^4); 360(1.89 × 10^4)	489	129	<0.001
	solid		513		0.0025
4-NEt_2-B	toluene	280(7.80 × 10^3); 346(8.02 × 10^4)	461	115	0.22
	CH_2Cl_2	273(2.00 × 10^4); 347(7.50 × 10^4)	482	135	0.13
	ethanol	269(4.05 × 10^3); 347(4.57 × 10^4)	494	147	0.015
	acetone	345(5.05 × 10^4)	464	119	0.24
	MeCN	270(6.78 × 10^3); 350(7.57 × 10^4)	494	144	0.003
	DMSO	277(1.04 × 10^4); 355(8.01 × 10^4)	494	139	0.001
	solid		499		0.25
5-OMe-B	toluene	281(2.29 × 10^4); 391(1.23 × 10^4)	520	129	0.14
	CH_2Cl_2	269(3.50 × 10^4); 388(1.38 × 10^4)	530	142	0.11
	ethanol	271(3.00 × 10^4); 383(1.18 × 10^4)	522	139	0.044
	acetone	385(1.18 × 10^4)	521	136	0.13
	MeCN	273(3.05 × 10^4); 384(1.29 × 10^4)	530	146	0.038
	DMSO	275(2.98 × 10^4); 380(1.57 × 10^4)	527	147	0.039
	solid		579		0.008
Naph-B	toluene	330(1.94 × 10^4); 372(1.63 × 10^4)	456	84	0.033
	CH_2Cl_2	332(2.70 × 10^4); 370(2.21 × 10^4)	455	85	0.078
	ethanol	328(2.68 × 10^4); 370(2.24 × 10^4)	459	89	0.011
	acetone	340(1.91 × 10^4); 373(2.14 × 10^4)	455	82	0.039
	MeCN	328(2.65 × 10^4); 371(2.39 × 10^4)	450	79	<0.001

DOI: 10.1021/acsomega.8b01504
ACS Omega 2018, 3, 8992−9002

Table 1. continued

	medium	λ_{abs}/nm (ε/dm^3 mol^{-1}cm^{-1})	λ_{em}/nm	Stokes shift/nm	Φ
Naph-B	DMSO	329(3.14 × 10^4); 373(3.17 × 10^4)	457	84	<0.001
	solid		495		0.11

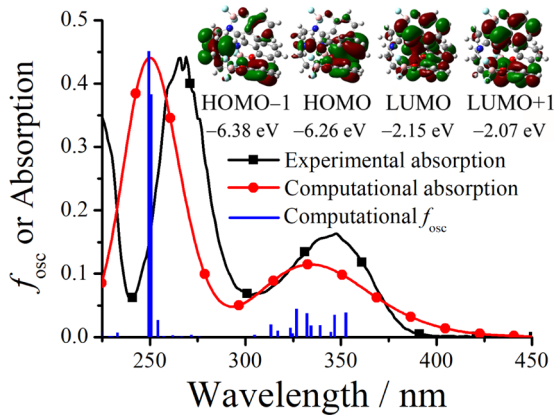

Figure 2. Computational and experimental (in CH_2Cl_2) absorption spectra, energy-level diagram, and Frontier molecular orbitals of **B**.

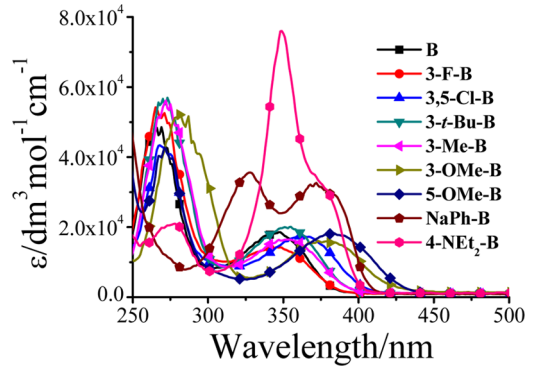

Figure 3. Absorption spectra of all of the B(III) complexes in CH_2Cl_2.

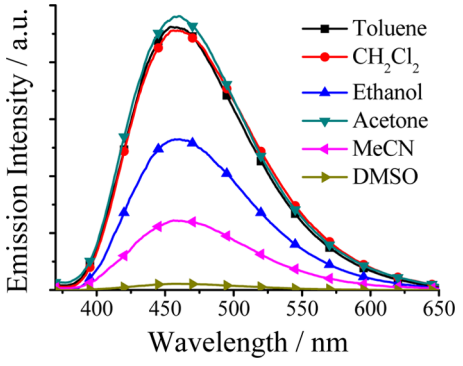

Figure 4. Emission spectra of **B** in different organic solvents (1.0 × 10^{-5} mol dm^{-3}).

complexes show an unusual solvent effect. For a usual solvent effect, high polar solvents would quench the fluorescence intensity with obvious red shifts in λ_{em}. For the B(III) complexes, high polar solvents, such as ethanol, MeCN, and DMSO, quench the fluorescence intensity with little red shifts in λ_{em} (see the later discussion).

In dilute CH_2Cl_2, the B(III) complexes with different substituents have various emission peaks (λ_{em}: 455−530 nm) and colors (blue, green, and green-yellow). The substituent effect of fluorescence spectra (Table 1 and Figure 6) is much different from that of absorption spectra (Figure 3). The presence of a π-extended system (**Naph-B**, λ_{em} = 455 nm) to the **B** (λ_{em} = 459 nm) leads to blue shifts in fluorescence spectra, but other substituents (**3-Me-B**, λ_{em} = 477 nm; **3-*t*-Bu-B**, λ_{em} = 470 nm; **3-F-B**, λ_{em} = 470 nm; **3,5-Cl-B**, λ_{em} = 488 nm; **4-NEt$_2$-B**, λ_{em} = 482 nm; **3-OMe-B**, λ_{em} = 517 nm; **5-OMe-B**, λ_{em} = 530 nm) result in red-shifted emission (Figure 6 and Table 1). Most of the solid-state B(III) complexes exhibit red-shifted fluorescence (λ_{em} up to 579 nm) compared with those solution samples, except **3-*t*-Bu-B** (λ_{em} = 461 and 470 nm in solid and CH_2Cl_2, respectively). These experimental results reveal that this substituent effect is a simple and useful tool to well tune λ_{em} and achieve RGB emission.

All fluorescence quantum yields (Table 1) of the B(III) complexes in solution and solid were measured by the optical dilute method with a standard of quinine sulfate (Φ_r = 0.55, quinine in 0.05 mol dm^{-3} sulfuric acid) and an integrating sphere, respectively. Although the complexes with a non-conjugated triethylamine linker have a small π-conjugated system, the fluorescence quantum yields of some B(III) complexes are unexpectedly high (Table 1). In dilute CH_2Cl_2, the presence of bulky hindering substituents of −*t*-butyl (**3-*t*-Bu-B**, Φ = 0.13) and −NEt$_2$ (**4-NEt$_2$-B**, Φ = 0.13) and π-extended system (**Naph-B**, Φ = 0.078) would improve fluorescence quantum yields (**B**, Φ = 0.064), but the introduction of −F (**3-F-B**, Φ = 0.034) and −Cl (**3,5-Cl-B**, Φ = 0.030) would bring adverse effects. A similar substituent effect was observed for the solid-state B(III) complexes. However, solid-state free tri-SSB ligands have a much different substituent effect in that the introduction of −F and −Cl would help improve AIE, but −*t*-butyl, −NEt$_2$, and π-extended systems would weaken AIE. This is further confirmed by the fact that the B(III) complexes and free ligands have different transition natures.

X-ray Single-Crystal Structures and Mechanism of Fluorescence. The molecule chemical structures and X-ray single-crystal arrangements play a key role for whether ACQ-or AIE-active materials.[63−67] To achieve a high fluorescence quantum yield, normal fluorescent materials usually need a planar π-conjugation and might suffer the ACQ problem consequently. On the other hand, AIE-active materials, such as propeller-type tetraphenylethene, usually are nonplanar π-conjugated molecules with not only strong intermolecular aromatic $H_{Ar}\cdots\pi$ hydrogen bonds but also weak intermolecular face-to-face $\pi-\pi$ interactions,[27,28] in which the former can ensure the elimination of the IRs and the latter would prevent the formation of excimer. For nonconjugated AIE-active free ligands of tri-SSBs, the restriction of C−C and C−N single bond rotations in the central alkyl chain bridges through some other noncovalent intermolecular interactions, such as N···H, O···H, C···H, F···H, Cl···H, and H···H, must be considered as well.[31]

It is interesting that the reported bi-/tri-SSB-based B(III) complexes[58,61] and free bi-/tri-SSB ligands[29−31] (Figure 1a) are ACQ- and AIE-active materials, respectively, but the tri-SSB-based B(III) complexes in this work emit strong

DOI: 10.1021/acsomega.8b01504
ACS Omega 2018, 3, 8992−9002

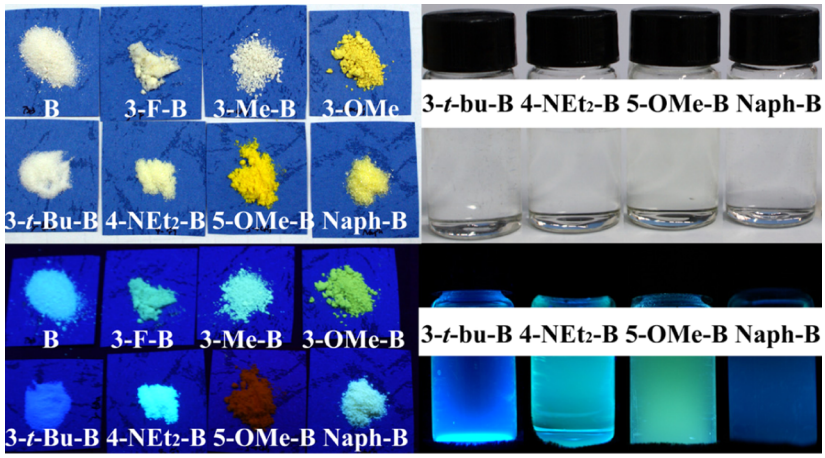

Figure 5. Photographs (top: under room light; bottom: under 360 nm UV light) of the selected complexes in solid state and CH_2Cl_2 (1.0×10^{-5} mol dm^{-3}).

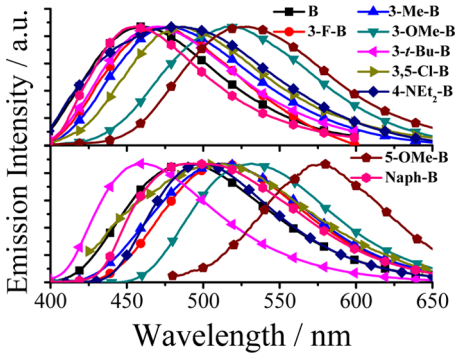

Figure 6. Normalized emission spectra of all of the complexes in CH_2Cl_2 (top, 1.0×10^{-5} mol dm^{-3}) and solid state (bottom).

fluorescence in both solution and solid state. To investigate the effect of molecular structures and arrangements, the X-ray single-crystal structures of **B** (CCDC: 1836233), **3,5-Cl-B** (CCDC: 1836234), and **4-NEt$_2$-B** (CCDC: 1836235) are depicted in Figures 7−9 and S1−S3 (in the Supporting Information). Unlike reported planar bi-/tri-SSB-based B(III) complexes,[58,61] the B(III) complexes are unusual tripodlike side-single-opening cages like free tri-SSB ligands[31] due to the stress from lone pair electrons of N atom in the triethylamine bridge (Figure 2).

As shown in Figure 7, the dihedral angles among three panels of π-conjugated iminomethylphenol are about 60°, resulting in no intramolecular face-to-face $\pi-\pi$ interactions (overlaps in π-conjugated units) in one **B** molecule. In dilute organic solution, it is obvious that the C−C and C−N single bonds in the central triethylamine bridge might be rotatable, which would afford a possible way to nonradiatively annihilate its excited states and quench the fluorescence consequently. However, there are many intramolecular hydrogen bonds between F atoms (BF_2) and H atoms ($H_{triethylamine}$: 2.329−2.822 Å; $H_{N=CH}$: 2.404−2.595 Å, Figure 7b), which would help block these IRs and lead to the presence of fluorescence in dilute organic solution. In the solid state, **B** molecules exhibit an edge-to-face spiral packing motif (Figure 7a), in which the opening directions of **B** molecular cages are in staggered form. Even though **B** molecules have a short interplanar distance (d) of 3.45 Å (Figure 7b), they are cross-stacking and result in weak intermolecular face-to-face $\pi-\pi$ interactions between two

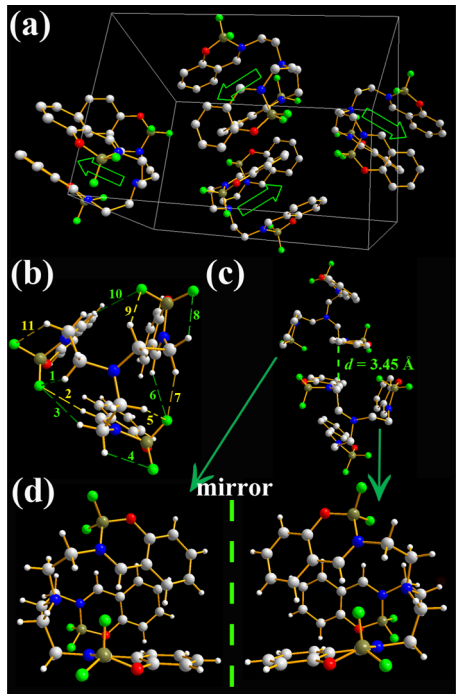

Figure 7. X-ray single-crystal structures and packing of **B** molecules: (a) packing in a unit cell (H atoms are omitted and green arrows indicate the opening direction of molecular cages); (b) intramolecular hydrogen bonds ($H_{triethylamine}$: 1 = 2.329 Å, 3 = 2.822 Å, 4 = 7 = 2.557 Å, 5 = 2.524 Å, 8 = 2.509 Å, 9 = 2.546 Å, 11 = 2.759 Å; $H_{N=CH}$: 2 = 2.458 Å, 6 = 2.404 Å, 10 = 2.595 Å); (c) intermolecular face-to-face $\pi-\pi$ interactions of the two close molecules (H atoms are omitted); and (d) enantiomers.

neighbor **B** molecules (Figure S1), which are beneficial to prevent the formation of excimer and achieve solid-state fluorescence. It is not surprising to find one pair of enantiomers (1:1) in the single crystals of **B** (Figure 7d) because the C−N and C−C single bonds cannot rotate freely in solid.[31,50] Since the intramolecular hydrogen bonds (Figure 2b) might help stabilize the existence of two enantiomers in dilute organic solution, it is possible to separate two enantiomers by chiral high-performance liquid chromatography. This is totally different from the enantiomers of free ligands.[31] The free ligands do not have such intramolecular

DOI: 10.1021/acsomega.8b01504
ACS Omega 2018, 3, 8992−9002

hydrogen bonds and thus the enantiomers of free ligands might be unstable to separate in dilute organic solution. Furthermore, we speculate that these intramolecular hydrogen bonds would be destroyed by high polar solvents through intermolecular hydrogen bonds between solvent and **B** molecules, and thus the fluorescence would be quenched by high polar solvents (Figure 4 and Table 1). This finding is in contrast to the phenomenon of polar solvent-induced fluorescence.[68,69]

Like **B** molecules, **3,5-Cl-B** molecules have a similar molecular structure and arrangement (Figure 8a). Many

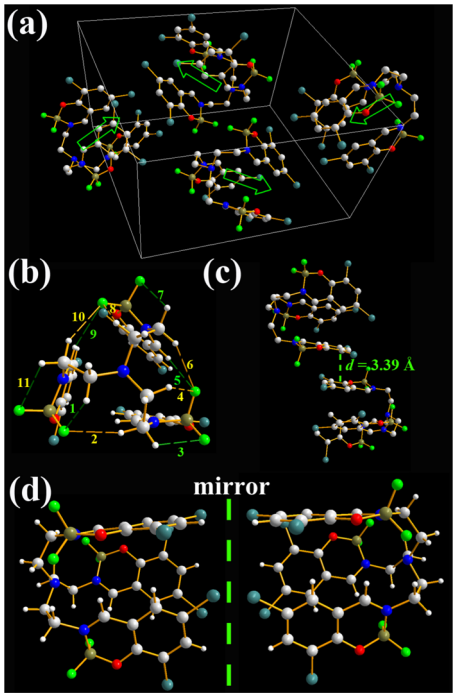

Figure 8. X-ray single-crystal structures and packing of **3,5-Cl-B-B** molecules: (a) packing in a unit cell (H atoms are omitted and green arrows indicate the opening direction of molecular cages); (b) intramolecular hydrogen bonds ($H_{triethylamine}$: 1 = 2.274 Å, 2 = 2.530 Å, 3 = 2.510 Å, 4 = 2.478 Å, 6 = 2.563 Å, 7 = 2.777 Å, 8 = 2.289 Å, 10 = 2.670 Å, 11 = 2.728 Å; $H_{N=CH}$: 5 = 2.282 Å, 9 = 2.593 Å); (c) intermolecular face-to-face $\pi-\pi$ interactions of the two close molecules (H atoms are omitted); and (d) enantiomers.

intramolecular hydrogen bonds ($H_{triethylamine}$: 2.274−2.777 Å; $H_{N=CH}$: 2.282−2.593 Å, Figure 8b) and two enantiomers (1:1) (Figure 8d) are also found in the two adjacent **3,5-Cl-B** molecules. However, **3,5-Cl-B** molecules show moderate intramolecular face-to-face $\pi-\pi$ interactions with a shorter d of 3.39 Å (Figures 8c and S2). Moreover, the density of **3,5-Cl-B** single crystals is 1.630 g cm^{-3}, which is much larger than that of **B** (1.456 g cm^{-3}) single crystals. The above factors indicate that **3,5-Cl-B** molecules are more likely to aggregate in both solution and solid state and have weaker fluorescence than **B** molecules consequently. Moreover, the electron-donating nature of −Cl substituents might also affect its fluorescence properties. This chlorination and fluorination effect for the B(III) complexes is much different from that for the free ligands.[31] For the free ligands, the chlorination and fluorination would help induce intermolecular F···H, Cl···H, or Cl···Cl interactions to enhance AIE.

Our previous works[29−31] demonstrated that bulky $-NEt_2$ and $-t$-Bu substituents might prevent the molecules from packing tightly, resulting in the absence of AIE from nonconjugated free SSB ligands. With bulky $-NEt_2$ substituents, **4-NEt_2-B** molecules have a similar molecular structure and arrangement (Figure 9a) as **B** molecules. Many

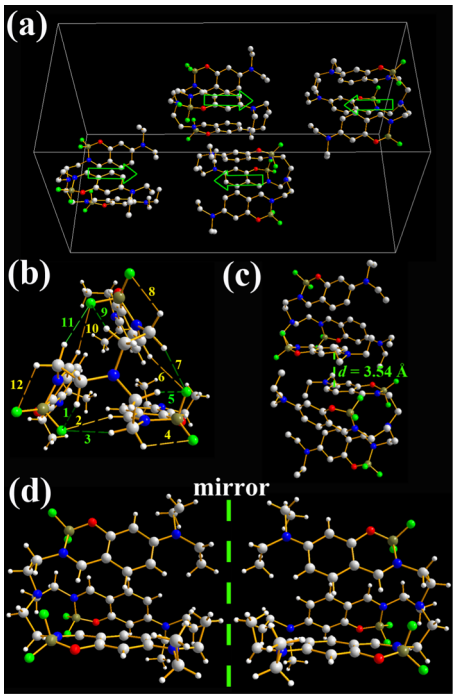

Figure 9. X-ray single-crystal structures and packing of **4-NEt_2-B** molecules: (a) packing in a unit cell (H atoms are omitted and green arrows indicate the opening direction of molecular cages); (b) intramolecular hydrogen bonds ($H_{triethylamine}$: 1 = 5 = 9 = 2.479 Å, 3 = 7 = 11 = 2.492 Å, 4 = 8 = 12 = 2.541 Å; $H_{N=CH}$: 2 = 6 = 10 = 2.672 Å); (c) intermolecular face-to-face $\pi-\pi$ interactions of the two close molecules (H atoms are omitted); and (d) enantiomers.

intramolecular hydrogen bonds (2.479−2.541 Å; $H_{N=CH}$: 2.672 Å, Figure 9b) and two enantiomers (Figure 9d) exist as well. However, the density (1.312 g cm^{-3}) and d (3.54 Å without intermolecular face-to-face $\pi-\pi$ interactions, Figures 9c and S3) of **4-NEt_2-B** single crystals is the smallest and largest, respectively, which reveal that the bulky $-NEt_2$ substituents would help prevent **4-NEt_2-B** molecules from aggregating to obtain the strongest fluorescence in both solution and solid state. A similar effect of bulky substituents is observed for **3-*t*-Bu-B** as well. Of course, we cannot exclude the possibility that the electron-donating nature of $-NEt_2$ substituents might also enhance its fluorescence.[61] There are B-level alerts in the checkCIF report of **4-NEt_2-B** due to the disorder of the $-NEt_2$ group in the single-crystal structures. Such disorder is quite common in terminal alkyl groups.[50]

The B(III) complexes have small π-conjugated systems but strong emission with large Stokes shifts, which are consistent with the characteristics of the reported pure organic phosphorescent compounds.[70] However, time-resolved emission spectra (Figure 10) reveal that the emission decay lifetime of **B** is 3.14 and 12.61 ns in dilute CH_2Cl_2 solution and solid, respectively. The emission decay lifetime of **4-NEt_2-B** is 10.3 and 22.3 ns in dilute CH_2Cl_2 solution and solid, respectively. This indicates that the emission of the B(III) complexes originates from fluorescence rather than phosphorescence. These relatively long emission decay lifetimes and large Stokes

DOI: 10.1021/acsomega.8b01504
ACS Omega 2018, 3, 8992−9002

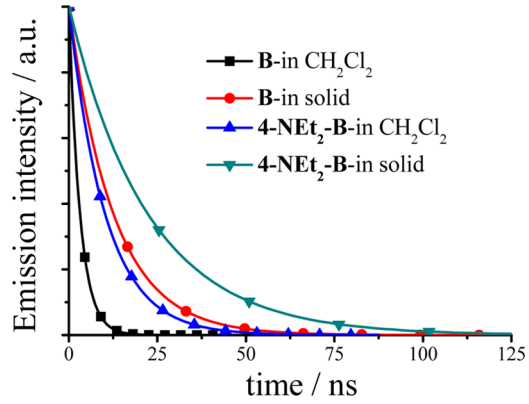

Figure 10. Time-resolved emission spectra of **B** and **4-NEt_2-B**.

shifts of B(III) complexes might be contributed by their transition nature of the ICT process (Figure 2).

Anion Host Properties. As our previous work,[31] the cagelike free ligands were used as anion hosts to detect anions through intermolecular hydrogen bonds, and thus we used B, **5-OMe-B**, and **3,5-Cl-B** to test their fluorescence responses upon adding different anions (Figures 11, S4, and S5). Various

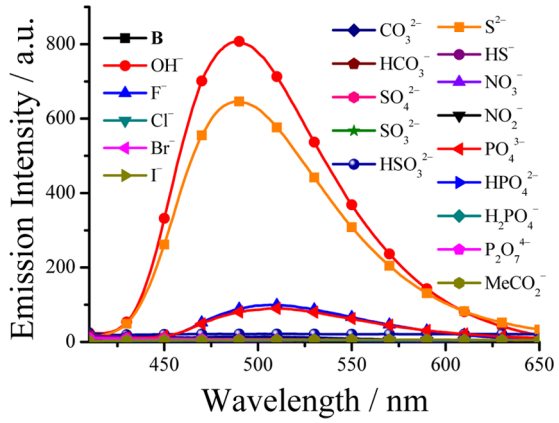

Figure 11. Emission spectra of **B** (2.0×10^{-5} mol dm^{-3} in DMSO, excited at 390 nm) upon the addition of 100 equiv of different anions.

sodium or potassium salts (1.0−0.10 mol dm^{-3} in water) were added to dilute dye solution (2.0×10^{-5} mol dm^{-3} in DMSO) by a microsyringe. The sensing performance would be much worse if other solvents, such as CH_2Cl_2, MeCN, EtOH, and MeOH, were used. As example, upon adding many anions, including OH^-, F^-, Cl^-, Br^-, I^-, NO_3^-, NO_2^-, CO_3^{2-}, HCO_3^-, S^{2-}, HS^-, SO_4^{2-}, SO_3^{2-}, HSO_3^-, PO_4^{3-}, HPO_4^{2-}, $H_2PO_4^-$, $P_2O_7^{4-}$, and $MeCO_2^-$, to dilute B DMSO solution, some of them, such as OH^- ($\Phi = 0.15$), S^{2-}, F^-, and PO_4^{3-}, would lead to turn on the fluorescence of B, but others will have little effects on the fluorescence (Figure 11). Similar fluorescence enhancements are observed upon adding different anions to dilute **5-OMe-B** solution (OH^-, $\Phi = 0.13$, Figure S4). However, **3,5-Cl-B** shows different fluorescence enhancements (Figure S5). Many anions, such as S^{2-} ($\Phi = 0.15$), PO_4^{3-}, F^-, CO_3^{2-}, HCO_3^-, $P_2O_7^{4-}$, $MeCO_2^-$, HPO_4^{2-}, HS^-, and SO_3^{2-}, would induce fluorescence enhancements. Under the same experimental conditions, the sensing performances of B and **3,5-Cl-B** are much different from those of free ligands,[31] which reveal that adding anions would not decompose the complexes to form the free ligands. We guess that the fluorescence could be regenerated by adding anions through intermolecular hydrogen bonds between the B(III) complexes and anions. These findings indicate that the B(III) complexes have potential applications in anion hosts/probes.

Living Cell Imaging. Since nonconjugated materials might have low cytotoxicity and good biocompatibility, we tried to use **4-NEt_2-B** and **3-Me-B** for the application of living cell imaging. The cervical cells were imaged by **4-NEt_2-B** and **3-Me-B** using a standard cell-staining protocol. As shown in Figure 12, incubated with the **4-NEt_2-B** and **3-Me-B**, over 90% cells are live, similar to those in the control experiments in the absence of the dyes, indicating that these dyes have little toxicity on the living cells. In the control experiments, cervical cells exhibit negligible background fluorescence, but intense intracellular green fluorescence is observed if cervical cells are incubated with **4-NEt_2-B** and **3-Me-B**.

CONCLUSIONS

In the present work, we report the nonconjugated trinuclear B(III) complexes that exhibit unique enantiomers with a tripodlike side-single-opening structure. The normal fluorescent B(III) complexes often suffer ACQ problem with narrow Stokes shifts. Although these B(III) complexes link with a nonconjugated triethylamine bridge, they display strong RGB fluorescence in both solution and solid due to the presence of strong intramolecular hydrogen bonds and the absence of intermolecular and intramolecular $\pi-\pi$ interactions. Moreover, they also have relatively long emission decay lifetimes and large Stokes shifts through the ICT transition process. Further studies on the separation of the enantiomers of B(III) complexes are currently under way in our cooperative laboratory. Therefore, we believe that these simple Schiff base-based nonconjugated trinuclear B(III) complexes provide a new paradigm in the design of nonconjugated fluorescent materials for developing advanced organic optoelectronic devices, florescent anion hosts/probes, chiral materials, cell imaging, and so on.

EXPERIMENTAL PROCEDURES

Materials and Instrumentation. All reagents were purchased from commercial suppliers and used without further purification. All of the ligands were prepared according to our previous report.[52] ^{1}H NMR (400 MHz) spectra were recorded in DMSO-d_6. Chemical shifts are reported in ppm using tetramethylsilane as internal standard. UV−vis absorption spectra were recorded using a U5100 (Hitachi) spectrophotometer with quartz cuvettes of 1 cm pathlength. Fluorescence spectra were obtained using an F-7000 Fluorescence spectrophotometer (Hitachi) at room temperature or 77 K (in liquid nitrogen). The photon multiplier voltage was 400 V. Samples in solution and powder were contained in 1 cm pathlength quartz cuvettes (3.5 mL volume) and quartz tube, respectively. The single crystals were obtained by a slow diffusion/evaporation of CH_2Cl_2/hexane solution at room temperature during about two weeks.

Measurement of Fluorescence Quantum Yield (Φ). The quantum yield of a solution sample was measured by the optical dilute method with a standard of quinine sulfate according to our previous report.[45] The quantum yield of a solid sample was measured by an integrating sphere.

Computational Details. The program Gaussian 09 was employed to perform DFT and TD-DFT calculations based on

DOI: 10.1021/acsomega.8b01504
ACS Omega 2018, 3, 8992−9002

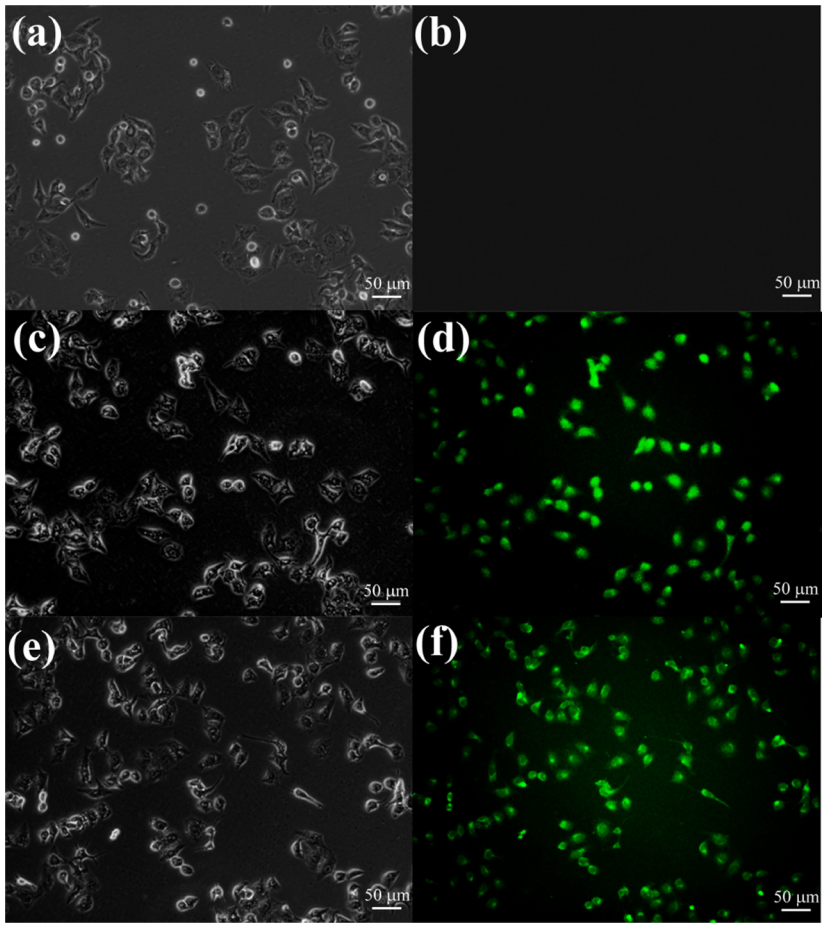

Figure 12. Brightfield (a, c, and e) and fluorescence (b, d, and f) images of cervical cells incubated without dye (a, b) and with the dyes of **3-Me-B** (c, d) and **4-NEt$_2$-B** (e and f).

the X-ray single-crystal structure of **B**. These included geometry optimizations of the singlet ground state and the triplet lowest-lying structures. TD-DFT was used to calculate 80 singlet−singlet transitions. CH_2Cl_2 was used as solvent in the TD-DFT calculations (pcm method). Geometries were optimized in the gas phase.

Cell Culture Methods and Imaging.[71] The imaging of HeLa cells was finished by Fluorescence Vertical Microscope LEICA DM2500. HeLa cells were cultured in Dulbecco's modified eagle medium supplemented with 10% fetal bovine serum, penicillin (100 units mL^{-1}), streptomycin (100 mg mL^{-1}), and 5% CO_2 at 37 °C. After removing the incubating media and rinsing with PBS for three times, the cells were incubated with the dye (1.0×10^{-5} mol dm^{-3}) in PBS for 2 h at room temperature. Then, the cells were washed three times with PBS and incubated with aqueous alkali for 20 min. At last, the cells were imaged with a confocal microscope.

Measurement of Anion Hosts. Various sodium or potassium salts (1.0−0.10 mol dm^{-3} in water) were added to dilute dye solution (2.0×10^{-5} mol dm^{-3} in DMSO) by a microsyringe. Fluorescence measurements were monitored at about 1 h after the addition of the anion to the dye solution at room temperature.

Synthesis of Complexes. The free tri-SSB ligands were reasonably easy to synthesize by the condensation of primary triethylamine with 3 equiv of salicylaldehyde precursor in ethanol under refluxing condition.[31] The mixture of salicyaldehyde or salicylaldehyde derivatives (3.1 mmol) and the corresponding triamine (1.0 mmol) in 20 mL of ethanol solution was refluxed at 78 °C for 5 h. After the reaction was complete, the mixture was cooled to 0 °C, and then the product in crystal or powder was collected by filtration.

The B(III) complexes were prepared by using BF_3−OEt_2 and tri-SSB ligands in toluene at 60 °C with excellent yields.[58] The free ligand (1 mmol) was dissolved in dry 20 mL of toluene. *N*,*N*-Diisopropylethylamine (0.5 mL) (10 mmol) was added, and the resulting mixture was stirred for 10 min at 60 °C, after which boron trifluoride diethyl etherate (10 mmol) was added dropwise. The final mixture was stirred for 5 h at 60 °C under a nitrogen atmosphere and then cooled to room temperature. CH_2Cl_2 (5 mL) was added, and the crude mixture was washed with water (3−2 mL). The organic layer was separated, dried over Na_2SO_4, and evaporated to dryness. The residue was purified by flash chromatography (CH_2Cl_2).

B (yield 80%) ^{1}H NMR (400 MHz, DMSO-d_6) δ 8.77 (s, 3H), 7.70−7.61 (m, 3H), 7.45 (dd, J = 7.8, 1.5 Hz, 3H), 7.01 (dd, J = 15.9, 8.0 Hz, 6H), 3.79 (t, J = 6.2 Hz, 6H), 3.02 (t, J = 6.6 Hz, 6H). ^{13}C NMR (101 MHz, DMSO-d_6) δ 167.45, 158.23, 138.50, 132.73, 120.59, 118.70, 115.78, 52.82, 50.43. HRMS (ESI): calculated for $C_{27}H_{27}B_3F_6N_4O_3$ [[M + Na]$^+$] 625.2164, found 625.2158. Anal. calcd. (found): C, 53.87 (53.79); H, 4.52 (4.53); N, 9.31 (9.29).

3-F-B (yield 79%) ^{1}H NMR (400 MHz, DMSO-d_6) δ 8.88 (s, 3H), 7.65−7.54 (m, 3H), 7.38 (d, J = 7.8 Hz, 3H), 7.01 (dd, J = 8.0, 4.4 Hz, 3H), 3.83 (t, J = 6.1 Hz, 6H), 3.05 (t, J = 6.6 Hz, 6H). ^{13}C NMR (101 MHz, DMSO-d_6) δ 167.42,

DOI: 10.1021/acsomega.8b01504
ACS Omega 2018, 3, 8992−9002

152.36, 149.91, 146.27 (d, J = 13.1 Hz), 128.21 (d, J = 3.4 Hz), 123.81 (d, J = 17.2 Hz), 120.35 (d, J = 6.5 Hz), 52.42, 50.42. HRMS (ESI): calculated for $C_{27}H_{24}B_3F_9N_4O_3$ [[M + Na]$^+$] 679.1882, found 679.1884. Anal. calcd (found): C, 49.44 (49.43); H, 3.69 (3.67); N, 8.54 (8.55).

3-Me-B (yield 83%) ^{1}H NMR (400 MHz, DMSO-d_6) δ 8.72 (s, 3H), 7.53 (d, J = 7.0 Hz, 3H), 7.29−7.22 (m, 3H), 6.89 (t, J = 7.6 Hz, 3H), 3.79 (t, J = 6.2 Hz, 6H), 3.01 (t, J = 6.5 Hz, 6H), 2.20 (s, 9H). ^{13}C NMR (101 MHz, DMSO-d_6) δ 167.48, 156.53, 138.87, 130.28, 127.23, 120.10, 115.13, 52.83, 50.26, 15.55. HRMS (ESI): calculated for $C_{30}H_{33}B_3F_6N_4O_3$ [[M + Na]$^+$] 667.2634, found 667.2627. Anal. calcd (found): C, 55.95 (55.92); H, 5.16 (5.15); N, 8.70 (8.68).

3-OMe-B (yield 82%) ^{1}H NMR (400 MHz, DMSO-d_6) δ 8.74 (s, 3H), 7.29 (dd, J = 8.0, 1.2 Hz, 3H), 7.00 (d, J = 1.3 Hz, 3H), 6.93 (d, J = 7.9 Hz, 3H), 3.81 (s, 9H), 3.79−3.75 (m, 6H), 2.99 (t, J = 6.3 Hz, 6H). ^{13}C NMR (101 MHz, DMSO-d_6) δ 167.87, 148.98, 148.44, 123.49, 120.31, 119.48, 115.82, 56.28, 52.71, 50.89. HRMS (ESI): calculated for $C_{30}H_{33}B_3F_6N_4O_6$ [[M + Na]$^+$] 715.2481, found 715.2489. Anal. calcd (found): C, 52.07 (52.10); H, 4.81 (4.79); N, 8.10 (8.12).

3-*t*-Bu-B (yield 70%) ^{1}H NMR (400 MHz, DMSO-d_6) δ 8.70 (s, 3H), 7.58 (dd, J = 7.7, 1.4 Hz, 3H), 7.18 (dd, J = 7.7, 1.4 Hz, 3H), 6.90 (t, J = 7.7 Hz, 3H), 3.79 (t, J = 6.0 Hz, 6H), 3.02 (t, J = 6.4 Hz, 6H), 1.37 (s, 27H). ^{13}C NMR (101 MHz, DMSO-d_6) δ 167.66, 157.09, 138.55, 134.96, 130.84, 120.18, 116.19, 52.82, 50.30, 34.96, 29.46. HRMS (ESI): calculated for $C_{39}H_{51}B_3F_6N_4O_3$ [[M + Na]$^+$] 793.4042, found 793.4038. Anal. calcd (found): C, 60.81 (60.80); H, 6.67 (6.69); N, 7.27 (7.28).

3,5-Cl-B (yield 80%) ^{1}H NMR (400 MHz, DMSO-d_6) δ 8.80 (s, 3H), 7.95 (d, J = 2.5 Hz, 3H), 7.61 (d, J = 2.5 Hz, 3H), 3.86 (t, J = 6.0 Hz, 6H), 3.05 (t, J = 6.3 Hz, 6H). ^{13}C NMR (101 MHz, DMSO-d_6) δ 166.66, 152.51, 136.83, 130.50, 123.80, 123.42, 117.28, 52.01, 50.33. HRMS (ESI): calculated for $C_{27}H_{21}B_3Cl_6F_6N_4O_3$ [[M + Na]$^+$] 828.9826, found 828.9815. Anal. calcd (found): C, 40.10 (40.13); H, 2.62 (2.60); N, 6.93 (6.92).

4-NEt$_2$-B (yield 88%) ^{1}H NMR (400 MHz, $CDCl_3$) δ 7.73 (s, 3H), 6.22 (s, 3H), 6.07 (s, 3H), 5.87 (s, 3H), 3.75 (s, 6H), 3.40 (q, J = 7.0 Hz, 12H), 2.89 (s, 6H), 1.22 (t, J = 7.0 Hz, 18H). HRMS (ESI): calculated for $C_{39}H_{54}B_3F_6N_7O_3$ [[M + Na]$^+$] 838.4369, found 838.4354. Anal. calcd (found): C, 57.45 (57.44); H, 6.68 (6.69); N, 12.03 (12.01).

5-OMe-B (yield 77%) ^{1}H NMR (400 MHz, DMSO-d_6) δ 8.72 (s, 3H), 7.25 (d, J = 3.2 Hz, 3H), 7.02 (d, J = 3.1 Hz, 3H), 6.96 (d, J = 9.1 Hz, 3H), 3.79 (t, J = 6.3 Hz, 6H), 3.73 (s, 9H), 3.03 (t, J = 6.6 Hz, 6H). ^{13}C NMR (101 MHz, DMSO-d_6) δ 167.07, 152.86, 152.61, 126.77, 119.67, 115.38, 113.75, 56.07, 52.72, 50.24. HRMS (ESI): calculated for $C_{30}H_{33}B_3F_6N_4O_6$ [[M + Na]$^+$] 715.2481, found 715.2467. Anal. calcd (found): C, 52.07 (52.09); H, 4.81 (4.80); N, 8.10 (8.11).

Naph-B (yield 75%) ^{1}H NMR (400 MHz, DMSO-d_6) δ 9.56 (s, 3H), 8.31 (d, J = 8.5 Hz, 3H), 8.18 (d, J = 9.1 Hz, 3H), 7.93 (d, J = 7.8 Hz, 3H), 7.68−7.61 (m, 3H), 7.49 (t, J = 7.4 Hz, 3H), 7.18 (d, J = 9.1 Hz, 3H), 3.94 (t, 6H), 3.17 (t, J = 6.9 Hz, 6H). ^{13}C NMR (101 MHz, DMSO-d_6) δ 163.22, 160.15, 139.90, 131.58, 129.62, 129.41, 127.96, 125.17, 120.92, 120.07, 108.11, 53.30, 50.66. HRMS (ESI): calculated for $C_{39}H_{33}B_3F_6N_4O_3$ [[M + Na]$^+$] 775.2634, found 775.2638. Anal. calcd (found): C, 62.28 (62.27); H, 4.42 (4.41); N, 7.45 (7.46).

■ ASSOCIATED CONTENT

Supporting Information

The Supporting Information is available free of charge on the ACS Publications website at DOI: 10.1021/acsomega.8b01504.

Side views of the face-to-face $\pi-\pi$ stacking interactions; fluorescence emission and NMR spectra (PDF)

Crystallographic data of 1836233 (**B**) (CIF)

Crystallographic data of 1836234 (**3,5-Cl-B**) (CIF)

Crystallographic data of 1836235 (**4-NEt$_2$-B**) (CIF)

■ AUTHOR INFORMATION

Corresponding Author

*E-mail: xianghaifeng@scu.edu.cn.

ORCID

Haifeng Xiang: 0000-0002-4778-2455

Author Contributions

§X.Z. and J.S. contributed equally to this work.

Notes

The authors declare no competing financial interest.

■ ACKNOWLEDGMENTS

This work was supported by the National Natural Science Foundation of China (no. 21372169) and Sichuan Science and Technology Program (no. 2018JY0559). We acknowledge the comprehensive training platform of the specialized laboratory of the College of Chemistry, Sichuan University, for material analysis. We would like to thank the Analytical & Testing Center of Sichuan University for CCD X-ray single-crystal diffractometer work and circular dichroism CD spectrometer work. We are grateful to Daibing Luo and Yani Xie for help with the single-crystal and circular dichroism measurements.

■ REFERENCES

(1) Valeur, B. *Molecular Fluorescence: Principles and Applications*; Wiley, 2002.

(2) Nolan, E. M.; Lippard, S. J. Tools and Tactics for the Optical Detection of Mercuric Ion. *Chem. Rev.* **2008**, *108*, 3443−3480.

(3) Kim, H. N.; Lee, M. H.; Kim, H. J.; Kim, J. S.; Yoon, J. A New Trend in Rhodamine-Based Chemosensors: Application of Spirolactam Ring-Opening to Sensing Ions. *Chem. Soc. Rev.* **2008**, *37*, 1465−1472.

(4) Zhao, Q.; Li, F. Y.; Huang, C. H. Phosphorescent Chemosensors Based on Heavy-Metal Complexes. *Chem. Soc. Rev.* **2010**, *39*, 3007−3030.

(5) Zhang, J. F.; Zhou, Y.; Yoon, J.; Kim, J. S. Recent Progress in Fluorescent and Colorimetric Chemosensors for Detection of Precious Metal Ions (Silver, Gold And Platinum Ions). *Chem. Soc. Rev.* **2011**, *40*, 3416−3429.

(6) Feng, Y.; Cheng, J. H.; Zhou, L.; Zhou, X. G.; Xiang, H. F. Ratiometric Optical Oxygen Sensing: A Review in Respect of Material Design. *Analyst* **2012**, *137*, 4885−4901.

(7) Yang, Y. M.; Zhao, Q.; Feng, W.; Li, F. Y. Luminescent Chemodosimeters for Bioimaging. *Chem. Rev.* **2013**, *113*, 192−270.

(8) Cheng, J. H.; Zhou, X. G.; Xiang, H. F. Fluorescent Metal Ion Chemosensors via Cation Exchange Reactions of Complexes, Quantum Dots, and Metal−Organic Frameworks. *Analyst* **2015**, *140*, 7082−7115.

(9) Mitschke, U.; Bauerle, P. The Electroluminescence of Organic Materials. *J. Mater. Chem.* **2000**, *10*, 1471−1507.

DOI: 10.1021/acsomega.8b01504
ACS Omega 2018, 3, 8992−9002

(10) Hung, L. S.; Chen, C. H. Recent Progress of Molecular Organic Electroluminescent Materials and Devices. *Mater. Sci. Eng., R* **2002**, *39*, 143−222.
(11) Mullen, K.; Mullen, U. S. *Organic Light Emitting Devices: Synthesis, Properties and Applications*; Wiley, 2006.
(12) *Highly Efficient OLEDs with Phosphorescent Materials*; Yersin, H., Ed.; Wiley, 2007.
(13) Xiang, H. F.; Cheng, J. H.; Ma, X. F.; Zhou, X. G.; Chruma, J. J. Near-infrared Phosphorescence: Materials and Applications. *Chem. Soc. Rev.* **2013**, *42*, 6128−6185.
(14) Slinker, J. D.; Rivnay, J.; Moskowitz, J. S.; Parker, J. B.; Bernhard, S.; Abruoac, H. D.; Malliaras, G. Electroluminescent Devices from Ionic Transition Metal Complexes. *J. Mater. Chem.* **2007**, *17*, 2976−2988.
(15) Costa, R. D.; Orti, E.; Bolink, H. J. Recent Advances in Light-Emitting Electrochemical Cells. *Pure Appl. Chem.* **2011**, *83*, 2115−2128.
(16) Fernandez-Moreira, V.; Thorp-Greenwood, F. L.; Coogan, M. P. Application of d_6 Transition Metal Complexes in Fluorescence Cell-Imaging. *Chem. Commun.* **2010**, *46*, 186−202.
(17) Zhao, Q.; Huang, C. H.; Li, F. Y. Phosphorescent Heavy-Metal Complexes for Bioimaging. *Chem. Soc. Rev.* **2011**, *40*, 2508−2524.
(18) Liang, J.; Tang, B. Z.; Liu, B. Specific Light-up Bioprobes based on AIEgen Conjugates. *Chem. Soc. Rev.* **2015**, *44*, 2798−2811.
(19) Wang, Y. F.; Zhang, T.; Liang, X. J. Aggregation-Induced Emission: Lighting up Cells Revealing Life! *Small* **2016**, *12*, 6451−6477.
(20) Birks, J. B. *Photophysics of Aromatic Molecules*; Wiley: New York, 1970.
(21) Ma, X. F.; Sun, R.; Cheng, J. H.; Liu, J. Y.; Gou, F.; Xiang, H. F.; Zhou, X. G. Fluorescence Aggregation-Caused Quenching versus Aggregation-Induced Emission: A Visual Teaching Technology for Undergraduate Chemistry Students. *J. Chem. Educ.* **2016**, *93*, 345−350.
(22) Tang, B. Z. New Structural Motifs for Solid Light Emitters. *Cutting-Edge Chemistry*; American Chemical Society, 2016. https://www.acs.org/content/acs/en/pressroom/cutting-edge-chemistry/new-structural-motifs-for-solid-light-emitters.html?cid=home_promo.
(23) Hong, Y.; Lam, J. W. Y.; Tang, B. Z. Aggregation-Induced Emission. *Chem. Soc. Rev.* **2011**, *40*, 5361−5388.
(24) Xing, C. M.; Lam, J. W. Y.; Qin, A.; Dong, Y.; Haussler, M.; Yang, W. T.; Tang, B. Z. Unique Photoluminescence from Nonconjugated Alternating Copolymer Poly[(maleic anhydride)-alt-(vinyl acetate)]. *ACS National Meeting Book of Abstracts*; Elsevier, 2007; Vol. *96*, p 418.
(25) Pucci, A.; Rausa, R.; Ciardelli, F. Aggregation-Induced Luminescence of Polyisobutene Succinic Anhydrides and Imides. *Macromol. Chem. Phys.* **2008**, *209*, 900−906.
(26) Mathew, M. S.; Sreenivasan, K.; Joseph, K. Hydrogen-Bond Assisted, Aggregation-Induced Emission of Digitonin. *RSC Adv.* **2015**, *5*, 100176−100183.
(27) Luo, J.; Xie, Z.; Lam, J. W. Y.; Cheng, L.; Chen, H.; Qiu, C.; Kwok, H. S.; Zhan, X.; Liu, Y.; Zhu, D.; Tang, B. Z. Aggregation-Induced Emission of 1-Methyl-1,2,3,4,5-pentaphenylsilole. *Chem. Commun.* **2001**, 1740−1741.
(28) Mei, J.; Leung, N. L. C.; Kwok, R. T. K.; Lam, J. W. Y.; Tang, B. Z. Aggregation-Induced Emission: Together We Shine, United We Soar! *Chem. Rev.* **2015**, *115*, 11718−11940.
(29) Cheng, J. H.; Li, Y. X.; Sun, R.; Liu, J. Y.; Gou, F.; Zhou, X. G.; Xiang, H. F.; Liu, J. Functionalized Salen Ligands Linking with Non-Conjugated Bridges: Unique and Colorful Aggregation-Induced Emission, Mechanism, and Applications. *J. Mater. Chem. C* **2015**, *3*, 11099−11110.
(30) Shen, G. Y.; Gou, F.; Cheng, J. H.; Zhang, X. H.; Zhou, X. G.; Xiang, H. F. Chiral and Non-Conjugated Fluorescent Salen Ligands: AIE, Anion Probes, Chiral Recognition of Unprotected Amino Acids, and Cell Imaging Applications. *RSC Adv.* **2017**, *7*, 40640−40649.
(31) Zhang, X. H.; Shen, G. Y.; Gou, F.; Cheng, J. H.; Zhou, X. G.; Xiang, H. F. Non-Conjugated Fluorescent Molecular Cages of Salicylaldehyde-Based Tri-Schiff Bases: AIE, Enantiomers, Mechanochromism, Anion Hosts/Probes, and Cell Imaging Properties. *Mater. Chem. Front.* **2017**, *1*, 1041−1050.
(32) Loudet, A.; Burgess, K. BODIPY Dyes and Their Derivatives: Syntheses and Spectroscopic Properties. *Chem. Rev.* **2007**, *107*, 4891−4932.
(33) Ulrich, G.; Ziessel, R.; Harriman, A. The Chemistry of Fluorescent Bodipy Dyes: Versatility Unsurpassed. *Angew. Chem., Int. Ed.* **2008**, *47*, 1184−1207.
(34) Boens, N.; Leen, V.; Dehaen, W. Fluorescent Indicators Based on BODIPY. *Chem. Soc. Rev.* **2012**, *41*, 1130−1172.
(35) Lu, H.; Mack, J.; Yang, Y.; Shen, Z. Structural Modification Strategies for the Rational Design of Red/NIR Region BODIPYs. *Chem. Soc. Rev.* **2014**, *43*, 4778−4823.
(36) Frath, D.; Massue, J.; Ulrich, G.; Ziessel, R. Luminescent Materials: Locking π-Conjugated and Heterocyclic Ligands with Boron(III). *Angew. Chem., Int. Ed.* **2014**, *53*, 2290−2310.
(37) Zhang, Z. L.; Bi, H.; Zhang, Y.; Yao, D. D.; Gao, H. Z.; Fan, Y.; Zhang, H. Y.; Wang, Y.; Wang, Y. Q.; Chen, Z. Y.; Ma, D. G. Luminescent Boron-Contained Ladder-Type π-Conjugated Compounds. *Inorg. Chem.* **2009**, *48*, 7230−7236.
(38) Zhang, Z. Y.; Zhang, H. Y.; Jiao, C. J.; Ye, K. Q.; Zhang, H. Y.; Zhang, J. Y.; Wang, Y. 2-(2-Hydroxyphenyl)benzimidazole-Based Four-Coordinate Boron Containing Materials with Highly Efficient Deep-Blue Photoluminescence and Electroluminescence. *Inorg. Chem.* **2015**, *54*, 2652−2659.
(39) Dhanunjayarao, K.; Mukundam, V.; Venkatasubbaiah, K. Tetracoordinate Imidazole-Based Boron Complexes for the Selective Detection of Picric Acid. *Inorg. Chem.* **2016**, *55*, 11153−11159.
(40) Baranov, M. S.; Lukyanov, K. A.; Borissova, A. O.; Shamir, J.; Kosenkov, D.; Slipchenko, L. V.; Tolbert, L. M.; Yampolsky, I. V.; Solntsev, K. M. Conformationally Locked Chromophores as Models of Excited-State Proton Transfer in Fluorescent Proteins. *J. Am. Chem. Soc.* **2012**, *134*, 6025−6032.
(41) Pais, V. F.; Alcaide, M. M.; Lopez-Rodriguez, R.; Collado, D.; Najera, F.; Perez-Inestrosa, E.; Alvarez, E.; Lassaletta, J. M.; Fernandez, R.; Ros, A.; Pischel, U. Strongly Emissive and Photostable Four-Coordinate Organoboron ÑC Chelates and Their Use in Fluorescence Microscopy. *Chem. - Eur. J.* **2015**, *21*, 15369−15376.
(42) Maeda, H.; Ito, Y. BF2 Complex of Fluorinated Dipyrrolyldiketone: A New Class of Efficient Receptor for Acetate Anions. *Inorg. Chem.* **2006**, *45*, 8205−8210.
(43) Zhang, G. Q.; Lu, J. W.; Sabat, M.; Fraser, C. L. Polymorphism and Reversible Mechanochromic Luminescence for Solid-State Difluoroboron Avobenzone. *J. Am. Chem. Soc.* **2010**, *132*, 2160−2162.
(44) Galer, P.; Korošec, R. C.; Vidmar, M.; Šket, B. Crystal Structures and Emission Properties of the BF2 Complex 1-Phenyl-3-(3,5-dimethoxyphenyl)-propane-1,3-dione: Multiple Chromisms, Aggregation- or Crystallization-Induced Emission, and the Self-Assembly Effect. *J. Am. Chem. Soc.* **2014**, *136*, 7383−7394.
(45) Cheng, J. H.; Wei, K. Y.; Ma, X. F.; Zhou, X. G.; Xiang, H. F. Synthesis and Photophysical Properties of Colorful Salen-Type Schiff Bases. *J. Phys. Chem. C* **2013**, *117*, 16552−16563.
(46) Cheng, J. H.; Zhang, Y. H.; Ma, X. F.; Zhou, X. G.; Xiang, H. F. Colorimetric and Fluorescent pH and Cu^{2+} Probes Induced by Photoisomerization of A Maleonitrile-Based Salen Ligand. *Chem. Commun.* **2013**, *49*, 11791−11793.
(47) Ma, X. F.; Cheng, J. H.; Liu, J. Y.; Zhou, X. G.; Xiang, H. F. Ratiometric Fluorescent pH Probes Based on Aggregation-Induced Emission-Active Salicylaldehyde Azines. *New J. Chem.* **2015**, *39*, 492−500.
(48) Cheng, J. H.; Ma, X. F.; Zhang, Y. H.; Liu, J. Y.; Zhou, X. G.; Xiang, H. F. Optical Chemosensors Based on Transmetalation of Salen-Based Schiff Base Complexes. *Inorg. Chem.* **2014**, *53*, 3210−3219.
(49) Cheng, J. H.; Gou, F.; Zhang, X. H.; Shen, G. Y.; Zhou, X. G.; Xiang, H. F. A Class of Multiresponsive Colorimetric and Fluorescent pH Probes via Three Different Reaction Mechanisms of Salen

DOI: 10.1021/acsomega.8b01504
ACS Omega 2018, 3, 8992−9002

Complexes: A Selective and Accurate pH Measurement. *Inorg. Chem.* **2016**, *55*, 9221−9229.
(50) Gou, F.; Cheng, J. H.; Zhang, X. H.; Shen, G. Y.; Zhou, X. G.; Xiang, H. F. Unusual Aggregation/Gelation-Induced Phosphorescence of Propeller-type Binuclear Platinum(II) Enantiomers. *Eur. J. Inorg. Chem.* **2016**, *2016*, 4862−4866.
(51) Song, J. T.; Wang, M.; Zhou, X. G.; Xiang, H. F. Unusual Circularly Polarized and Aggregation-Induced Near-Infrared Phosphorescence of Helical Platinum(II) Complexes with Tetradentate Salen Ligands. *Chem. Eur. J.* **2018**, *24*, 7128−7132.
(52) Riddle, J. A.; Lathrop, S. P.; Bollinger, J. C.; Lee, D. Schiff Base Route to Stackable Pseudo-Triphenylenes: Stereoelectronic Control of Assembly and Luminescence. *J. Am. Chem. Soc.* **2006**, *128*, 10986−10987.
(53) Hou, Q.; Zhao, L.; Zhang, H.; Wang, Y.; Jiang, S. Synthesis and Luminescent Properties of Two Schiff-Base Boron Complexes. *J. Lumin.* **2007**, *126*, 447−451.
(54) Frath, D.; Azizi, S.; Ulrich, G.; Retailleau, P.; Ziessel, R. Facile Synthesis of Highly Fluorescent Boranil Complexes. *Org. Lett.* **2011**, *13*, 3414−3417.
(55) Dhanunjayarao, K.; Mukundam, V.; Ramesh, M.; Venkatasubbaiah, K. Synthesis and Optical Properties of Salicylaldimine-Based Diboron Complexes. *Eur. J. Inorg. Chem.* **2014**, 539−545.
(56) Dobkowski, J.; Wnuk, P.; Buczyńska, J.; Pszona, M.; Orzanowska, G.; Frath, D.; Ulrich, G.; Massue, J.; Mosquera-Vázquez, S.; Vauthey, E.; Radzewicz, C.; Ziessel, R.; Waluk, J. Substituent and Solvent Effects on the Excited State Deactivation Channels in Anils and Boranils. *Chem. - Eur. J.* **2015**, *21*, 1312−1327.
(57) Gong, P.; Yang, H.; Sun, J.; Zhang, Z.; Sun, J.; Xue, P.; Lu, R. Salicylaldimine Difluoroboron Complexes Containing Tert-Butyl Groups: Nontraditional π-Gelator and Piezofluorochromic Compounds. *J. Mater. Chem. C* **2015**, *3*, 10302−10308.
(58) Frath, D.; Benelhadj, K.; Munch, M.; Massue, J.; Ulrich, G. Polyanils and Polyboranils: Synthesis, Optical Properties, and Aggregation-Induced Emission. *J. Org. Chem.* **2016**, *81*, 9658−9668.
(59) Urban, M.; Durka, K.; Jankowski, P.; Serwatowski, J.; Luliński, S. Highly Fluorescent Red-Light Emitting Bis(boranils) Based on Naphthalene Backbone. *J. Org. Chem.* **2017**, *82*, 8234−8241.
(60) Zhou, Y.; Kim, J. W.; Kim, M. J.; Son, W. J.; Han, S. J.; Kim, H. N.; Han, S.; Kim, Y.; Lee, C.; Kim, S. J.; Kim, D. H.; Kim, J. J.; Kim, D. H. Novel Bi-Nuclear Boron Complex with Pyrene Ligand: Red-Light Emitting as well as Electron Transporting Material in Organic Light-Emitting Diodes. *Org. Lett.* **2010**, *12*, 1272−1275.
(61) Guieu, S.; Cardona, F.; Rocha, J.; Silva, A. M. S. Luminescent Bi-Metallic Fluoroborate Derivatives of Bulky Salen Ligands. *New J. Chem.* **2014**, *38*, 5411−5414.
(62) Wei, P. R.; Atwood, D. A. Syntheses and Reactions of Saltren-Group 13 Complexes. *J. Organomet. Chem.* **1998**, *563*, 87−93.
(63) Gu, X. G.; Zhao, E. G.; Zhao, T.; Kang, M. M.; Gui, C.; Lam, J. W. Y.; Du, S. W.; Loy, M. M. T.; Tang, B. Z. A Mitochondrion-Specific Photoactivatable Fluorescence Turn-On AIE-Based Bioprobe for Localization Super-Resolution Microscope. *Adv. Mater.* **2016**, *28*, 5064−5071.
(64) Li, Q. Q.; Li, Z. The Strong Light-Emission Materials in the Aggregated State: What Happens from a Single Molecule to the Collective Group. *Adv. Sci.* **2017**, *4*, No. 1600484.
(65) Song, Y. C.; Zong, L. Y.; Zhang, L. Y.; Li, Z. To form AIE Product With the Target Analyte: A New Strategy for Excellent Fluorescent Probes, and Convenient Detection of Hydrazine in Seconds With Test Strips. *Sci. China: Chem.* **2017**, *60*, 1596−1601.
(66) Gu, X. G.; Kwok, R. T. K.; Lam, J. W. Y.; Tang, B. Z. AIEgens for biological process monitoring and disease theranostics. *Biomaterials* **2017**, *146*, 115−135.
(67) Gu, X. G.; Zhang, X. Y.; Ma, H. L.; Jia, S. R.; Zhang, P. F.; Zhao, Y. J.; Liu, Q.; Wang, J. G.; Zheng, X. Y.; Lam, J. W. Y.; Ding, D.; Tang, B. Z. Corannulene-Incorporated AIE Nanodots with Highly Suppressed Nonradiative Decay for Boosted Cancer Phototheranostics In Vivo. *Adv. Mater.* **2018**, *30*, No. 1801065.
(68) McDonald, L.; Wang, J. F.; Alexander, N.; Li, H.; Liu, T. B.; Pang, Y. Origin of Water-Induced Fluorescence Turn-On from a Schiff Base Compound: AIE or H-Bonding Promoted ESIPT. *J. Phys. Chem. B* **2016**, *120*, 766−772.
(69) Wang, M.; Cheng, C. Q.; Song, J. T.; Wang, J.; Zhou, X. G.; Xiang, H. F.; Liu, J. Multiple Hydrogen Bonds Promoted ESIPT and AIE-active Chiral Salicylaldehyde Hydrazide. *Chin. J. Chem.* **2018**, *36*, 698−707.
(70) Mukherjee, S.; Thilagar, P. Recent Advances in Purely Organic Phosphorescent Materials. *Chem. Commun.* **2015**, *51*, 10988−11003.
(71) Liu, J. Y.; Cheng, J. H.; Ma, X. F.; Zhou, X. G.; Xiang, H. F. Photophysical properties and pH sensing applications of luminescent salicylaldehyde derivatives. *Res. Chem. Intermed.* **2016**, *42*, 5027−5048.

DOI: 10.1021/acsomega.8b01504
ACS Omega 2018, 3, 8992−9002